

3,4-dihydroxyacetophenone inhibits hypoxia-associated human pulmonary artery smooth muscle cell proliferation by reducing Ca^{2+} influx

Chunlong Lin, Caixia Li, Jianping Zhao, Wang Ni, Jizu Yi

¹Respiratory Department of the Second Hospital of Yueyang, Hunan Normal University, Yueyang, East Road of Baling, Hunan, China

²Department of Chemistry and Chemical Engineering, Hunan Institute of Science and Technology, Yueyang, Hunan, China

Abstract: The present study aimed to assess the effects of 3,4-dihydroxyacetophenone (DHAP) on human pulmonary artery smooth muscle cells (HPASMCs). HPASMCs were divided into the normoxia group (NG), hypoxia group (HG), and hypoxia and 0.6×10^{-4} mol/L (HD1), 1.9×10^{-4} mol/L (HD2) and 6.0×10^{-4} mol/L (HD3) DHAP treatment groups. Cell cycle was analyzed by flow-cytometrically. HPASMC growth was examined by the proliferating cell nuclear antigen (PCNA) and MTT assays. Intracellular Ca^{2+} ($[\text{Ca}^{2+}]_i$) was measured by laser scanning confocal microscopy. Compared with the NG, the HG showed significantly increased HPASMC proliferation ($P < 0.05$); meanwhile, cells treated with DHAP showed decreased proliferation compared with the HG ($P < 0.05$). Hypoxia enhanced cell cycle progression and DHAP partly restored cell cycle distribution toward the status of NG cells. Furthermore, CDK2 levels were markedly increased in hypoxic cells ($P < 0.05$), while DHAP treatment starkly decreased CDK2 levels in comparison with the HG ($P < 0.05$). Moreover, hypoxia increased intracellular $[\text{Ca}^{2+}]_i$ levels compared with normoxia ($P < 0.05$); meanwhile, DHAP treatment decreased $[\text{Ca}^{2+}]_i$ compared with the HG ($P < 0.05$). These findings suggested that DHAP inhibits hypoxia-induced proliferation of HPASMCs involving $[\text{Ca}^{2+}]_i$ reduction. Therefore, DHAP should be considered an ideal candidate for the prevention and/or treatment of hypoxia-associated pulmonary hypertension and pulmonary vascular remodeling.

Keywords: 3,4-dihydroxyacetophenone, pulmonary artery smooth muscle cell, hypoxia, cell cycle, pulmonary hypertension, pulmonary vascular remodeling.

INTRODUCTION

Chronic obstructive pulmonary disease (COPD) represents a major threat to human health because of high prevalence, morbidity and mortality, especially in developing countries (Diaz-Guzman and Mannino, 2014, Foo *et al.*, 2016, Islam *et al.*, 2014). COPD induces pulmonary vasoconstriction that leads to pulmonary hypertension and pulmonary heart disease, secondary respiratory failure and eventually death (Disease, 2015). Pulmonary artery hypertension (PAH) represents a disease with multiple etiologies and is developed by the hallmark pathological features that include smooth muscle cell proliferation, inflammation and pulmonary vascular remodeling (Magne *et al.*, 2015, McLaughlin *et al.*, 2015). PAH complicates COPD in a large proportion of patients (Disease, 2015).

Endothelial dysfunction is now considered to have a critical function in PAH pathogenesis in COPD, and may result from hypoxemia (Polverino *et al.*, 2018, Zangiabadi *et al.*, 2014). Pulmonary vessel remodeling is characterized by intimal enlargement with smooth muscle cell proliferation, medial hypertrophy, arteriolar muscularization and endothelial cell proliferation, leading to permanent structural and functional alterations of

vessels (Stenmark *et al.*, 2006, Sun and Chan, 2018). Uncontrolled human pulmonary artery smooth muscle cell (HPASMC) growth represents a major factor triggering vascular remodeling in hypoxia-related pulmonary hypertension and is characterized by increased proliferation, hypertrophy, matrix protein production and cell recruitment (Wilson *et al.*, 2015). Ultimately, this causes the right heart to increase blood pressure for overcoming vascular resistance increase (Sun *et al.*, 2018, Wilson *et al.*, 2015). With disease progression, cor pulmonale might develop, with the five-year survival rate in such cases estimated at 20-36 % (Burger 2009, Park, *et al.*, 2015).

Ca^{2+} signaling in PSMCs has a critical function in PAH development and progression (Firth, *et al.*, 2013, Smith *et al.*, 2015). Indeed, hypoxia leads to decreased expression of K_v channels, membrane depolarization, voltage-dependent Ca^{2+} channel activation and Ca^{2+} accumulation within the cells (Firth *et al.*, 2013, Smith *et al.*, 2015). Contractions of PSMCs may also be induced by RhoA/Rho kinase-mediated Ca^{2+} sensitization (Firth, *et al.*, 2013, Smith, *et al.*, 2015). In addition, increased intracellular Ca^{2+} ($[\text{Ca}^{2+}]_i$) activates PSMC proliferation (Herbert, *et al.*, 2018). However, how hypoxia induces PAH remains unknown and requires further investigation. 3,4-dihydroxyacetophenone (DHAP; $\text{C}_8\text{H}_8\text{O}_3$; molecular weight, 152.15 Da) is an active molecule extracted from

*Corresponding author: e-mail: lclmd@sina.com

Folium Ilex Pubescens, a Chinese herb traditionally used for the treatment of coronary heart disease. Previous studies have shown that DHAP dilates coronary arteries, lowers myocardial oxygen consumption, improves myocardial microcirculation, prevents platelet aggregation and suppresses arrhythmia. DHAP has potential for treating coronary heart disease (Lin *et al.*, 1995, Lin, 2008). Farman *et al.* (Farman *et al.*, 1994) demonstrated that DHAP decreases hypoxic vasoconstriction in pulmonary artery rings. A previous study in dogs revealed that DHAP could decrease the responses of pulmonary and systemic blood vessels to hypoxia (Ullah *et al.*, 1995). In addition, DHAP down regulates monocyte chemo attractant protein-1 (MCP-1) in smooth muscle cells (Jiang *et al.*, 2009). However, the underlying mechanisms are unknown.

Therefore, this work aimed to assess DHAP's effects on human PASMC proliferation, cell cycle distribution, Proliferating cell nuclear antigen (PCNA) expression and $[Ca^{2+}]_i$. Our results showed that DHAP inhibited hypoxia-induced PASMC proliferation, suggesting that it might constitute a therapeutic candidate for PAH and associated diseases as well as further complications observed in COPD.

MATERIALS AND METHODS

Cell culture and treatment

HPASMCs were obtained from non-cancerous lung portions of four patients with lung cancer (aged 43-56 years; three males and 1 female; 3 and 1 cases of tumor-node-metastasis (TNM) stages I and II, respectively) who underwent partial lung resection. No patient was administered radiotherapy or chemotherapeutics pre-surgery. All authors declare that each patient provided signed informed consent for publishing any findings and related images. The present study was approved by the institutional ethics committee.

Cell culture was performed in the adherent format (Sue and Zane, 1987), in Dulbecco's modified Eagle's medium (DMEM) (HyClone, USA) containing 20% fetal bovine serum (FBS) (HyClone) and 10mM HEPES (pH 7.4), 100 U/ml penicillin G and 0.1mg/mL streptomycin. Cells at passages 3 to 8 were assessed. HPASMC confirmation was performed by hematoxylin & eosin (H&E) staining, immunocytochemistry for α -smooth muscle actin (α -SMA) detection using a specific mouse anti-human polyclonal antibody (Santa Cruz Biotechnology, USA) (Sue *et al.*, 1987), and immunofluorescence staining of calponin-1 (Morgan and Gangopadhyay, 2001).

HPASMCs were plated at 10^5 cells/mL in 50mL-culture flasks

After cells grew to 70-80% confluence, they were serum-starved for 24 hours, and incubated in medium with 10%

FBS for 24h. Five cell groups were set up: normoxia group (NG; 20% O₂, 5% CO₂ and 75% N₂); hypoxia group (HG; 5% O₂, 5% CO₂ and 90% N₂ in a hypoxia incubator [Galaxy Rs Biotech; New Brunswick Scientific, Edison, NJ, USA]) and hypoxia and 0.6×10^{-4} mol/L (HD1), 1.9×10^{-4} mol/L (HD2) and 6.0×10^{-4} mol/L (HD3) DHAP (Beijing Institute of Pharmaceutical Industry, China) treatment groups (CL Lin, 2008). After continuous incubation for 24h, HPASMCs were collected for analyses. Movat's pentachrome and Type III collagen staining assays were used to evaluate cell structure post-treatment.

Calponin-1 immunofluorescence

Cells were grown on sterile glass slides overnight at 37°C and fixed with 10% formaldehyde. Slides were rinsed with phosphate-buffered saline (PBS)-Tween 20, blocked with normal serum and incubated with FITC-calponin-1 primary antibodies (Santa Cruz Biotechnology) for 1h in ambient conditions or overnight at 4°C. Then, slides were rinsed with PBS and added biotinylated secondary antibodies for 30 min incubation in ambient conditions. After rinsing with PBS-Tween, FITC-Avidin D was added for 30 min at ambient temperature away from light. Finally, slides were counterstained with DAPI.

MTT assay

HPASMCs were plated at 10^4 cells/well in 96 well-plates and treated according to grouping. 3-(4,5-dimethylthiazol-2-yl)-2,5-diphenyltetrazolium bromide (MTT) (5mg/ml) was supplemented (20 μ l/well) following 24h of incubation. After 4 h incubation at 37°C, the medium was carefully removed and dimethyl-sulfoxide (150 μ l/well) was used to dissolve the formazan crystals. Optical density was measured at 490 nm on a micro plate reader.

Cell cycle analysis by flow cytometry

At the end of treatment, cells were detached with 0.25% trypsin and washed by centrifugation at room temperature and 1500 \times g for 10min. They were then re-suspended to 10^6 cell/mL in PBS (pH 7.2-7.4) and submitted to centrifugation at 1500 \times g (8min; ambient temperature). Cell fixation was performed using precooled 70% ethanol for 18h (-20°C), followed by treatment with 50 μ L of RNAase in ambient conditions for 30min. Next, 50 μ L of 10% propidium iodide (PI) (Thermo Fisher Scientific, USA) and 1% Triton X-100 were added for 30 min in ambient conditions. The cell proportions in the G0/G1, S and G2/M phases, as well as at the sub-G1 (apoptosis) stage were assessed on a FAC Sort Flow Cytometer (BD Bioscience, USA) using the Cell Quest software.

Total protein extraction and immunoblot

HPASMC lysis was carried out with slightly modified radioimmunoprecipitation assay (RIPA) buffer (50mM HEPES, 0.15M NaCl, 2mM EDTA, 0.1% NP-40, 0.05% sodium deoxycholate, 1mM Na₃VO₄, 40mM NaF and

10mM Sodium pyrophosphate; pH 7.2) (Beyotime Institute of Biotechnology, China), followed by centrifugation at 15,000×g at room temperature for 15 min. Protein amounts in the supernatant were measured by the bicinchonic acid (BCA) method (Beyotime Institute of Biotechnology). Equal amounts of proteins (90µg) were resolved by 10% SDS-polyacrylamide gel electrophoresis (SDS-PAGE) and electro-transferred onto nitrocellulose membranes (Pierce Chemical, USA). After blocking, the membranes were incubated with anti-PCNA (Santa Cruz Biotechnology) and anti-cyclin-dependent kinase 2 (CDK2) (Proteintech Group Inc., USA). Protein bands were detected with an ECL kit (Beyotime) and quantified using the Quantity One software (Bio-Rad, USA).

Intracellular calcium

HPASMCs with high viability were selected, washed with PBS containing no calcium and incubated with Fluo-3 AM (5mM) (AAT Bioquest, USA) in the dark for 30 min. The residual dye was removed by three washes with Hanks solution. Then, slides were covered and placed in stainless steel chambers, followed by Hanks solution addition. A laser scanning confocal microscope (Leica Microsystems, Germany) was used to monitor fluorescence changes upon treatment of HPASMCs with the respective DHAP concentrations for 24 h. Intracellular Ca^{2+} fluorescence intensity (FI) was acquired by laser scanning confocal microscopy. At room temperature, cells were scanned every 5s and signal intensity was determined with Image-Pro Plus 5.1 (Media Cybernetics, USA). The mean of 5 measurements was used to represent $[Ca^{2+}]_i$.

Ethical approval

All authors declare that each patient provided signed informed consent for publishing any findings and related images. The present study was approved by the Institutional Ethics Committee.

STATISTICAL ANALYSIS

Statistical analyses were carried out with SPSS 17.0 (SPSS, USA). Continuous data are mean ± standard deviation (SD) and were assessed by ANOVA with the SNK post-hoc test. Two-sided $P < 0.05$ indicated statistical significance.

RESULTS

Identification of HPASMCs

On immunocytochemical images, HPASMCs appeared as spindle-shaped with an oval nucleus in the center, notable nucleoli, and the “hill and valley” feature (fig. 1A). HPASMCs were positive for both α -SMA (fig. 1B) and calponin-1 (fig. 1C). In this study, these three characteristics were used to identify HPASMCs.

Effects of DHAP on hypoxia-induced HPASMC proliferation and pulmonary vascular remodeling

Based on the MTT assay, proliferation of HG cells was higher than that of the NG group ($P < 0.05$); meanwhile, DHAP treatment decreased cell proliferation in comparison with the NG and HG groups (all $P < 0.05$) (fig. 2A). Fig. 2B shows that HG cells had higher PCNA levels compared with NG counterparts and DHAP treatment resulted in decreased PCNA levels. Moreover, the expression of Ki67 was analyzed and the results were in line with those of PCNA and MTT assays (fig. 2C). The effects of DHAP on pulmonary vascular remodeling were also determined by the Movat's and type III collagen staining methods. As depicted in fig. 2D-E, nuclear and elastic fibers as well as type III collagen expression were decreased.

Effect of DHAP on cell cycle distribution in HPASMCs under hypoxia

Flow cytometry and PI staining showed that hypoxia induced a shift from G0/G1 toward S and G2/M ($P < 0.05$) (fig. 3A). DHAP partly restored the cell cycle distribution towards that of NG cells, but significant differences remained (fig. 3A).

As shown in fig. 3B, hypoxia increased CDK2 protein levels ($P < 0.05$), which were dose-dependently decreased by DHAP ($P < 0.05$).

Effects of DHAP on $[Ca^{2+}]_i$ in HPASMCs under hypoxia

Fig. 4A shows representative fluorescence images used to determine $[Ca^{2+}]_i$. Hypoxia increased $[Ca^{2+}]_i$ compared with normoxia ($P < 0.05$), while DHAP decreased these values ($P < 0.05$) (fig. 4B).

DISCUSSION

This study assessed DHAP's effects on HPASMCs and explored the potential mechanisms of hypoxia-induced HPASMC proliferation. DHAP is one of the active compounds extracted from *Folium Ilex Pubescens*, which was reported to activate blood circulation (Lin et al., 1995, Lin, 2008). Previous studies showed that DHAP decreases pulmonary vascular resistance and reduces blood viscosity (Lewiz et al., 2016, Lin et al., 1995, Lin 2008). Interestingly, systemic arterial blood pressure and arterial blood gas are not affected by DHAP, irrespective of concentrations; these characteristics make DHAP an attractive molecule with potential for new drug development (Lewis et al., 2016, Lin et al., 1995, Lin 2008).

CDK2-cyclin A belongs to cyclin-dependent kinases, which control the cell cycle in eukaryotes. CDK2 has a critical function in G1 to S transition (Bertoli et al., 2013). Liao et al. (2001) showed CDK2 over expression markedly enhances CDK4 and cyclin (A, D3, and E)

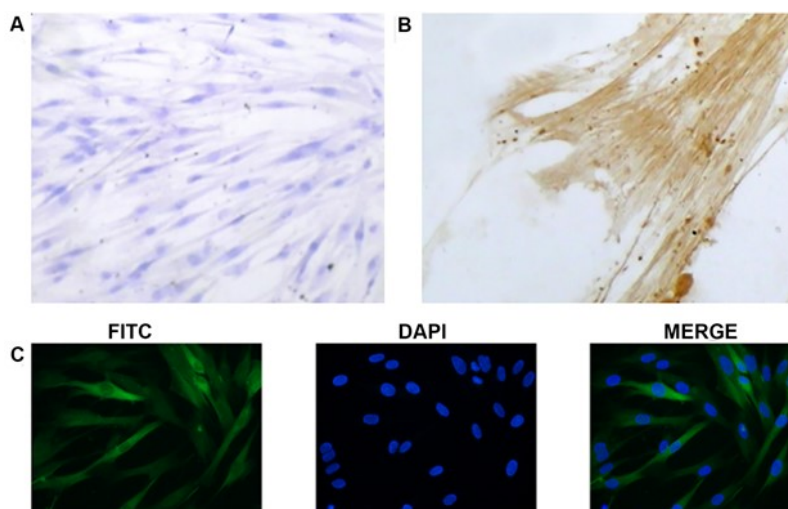


Fig. 1: Identification of human pulmonary artery smooth muscle cells (HPASMCs). (A) The morphology of HPASMCs assessed by H&E staining revealed the characteristic “hill and valley” and oval shape ($\times 100$). (B) The protein levels of α -smooth muscle actin (α -SMA) in HPASMCs were assessed by immunocytochemistry using the diaminobenzidine (DAB) method ($\times 400$). (C) Immunofluorescence staining of calponin-1 in HPASMCs ($\times 200$). Green, FITC; blue (nuclei), DAPI.

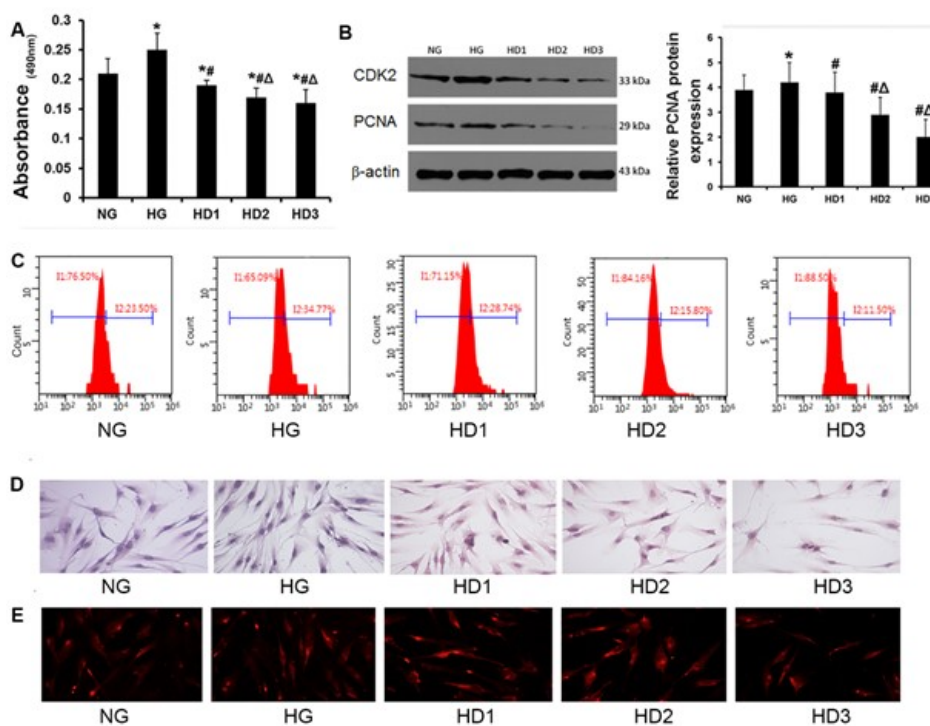


Fig. 2: Effect of 3,4-dihydroxyacetophenone (DHAP) on cell proliferation in HPASMCs under hypoxia. Cells were divided into five groups, including the normoxia group (NG), hypoxia group (HG) and hypoxia and 0.6×10^{-4} mol/L (HD1), 1.9×10^{-4} mol/L (HD2), and 6.0×10^{-4} mol/L (HD3) DHAP treatment groups. (A) Cell proliferation was assessed by the MTT assay. Data are absorbance at 490 nm. (B) PCNA protein expression was determined by Western blot, with β -actin as an internal control. Data are mean \pm standard deviation (SD). * $P < 0.05$ vs. NG; # $P < 0.05$ vs. HG; $\Delta P < 0.05$ vs. HD1. (C) Flow cytometry analysis of five groups of cells (NG, HG, HD-1, HD-2 and HD-3) was performed with another cell proliferation marker, Ki67 using PE anti-human Ki-67 Antibody (BioLegend catalog# 350504). Cell proliferation was decreased in hypoxic cells treated with DHAP compared with the HG group. Effects of DHAP on pulmonary vascular remodeling analyzed by Movat’s pentachrome (D) and type III collagen (E) staining. The results showed that nuclei and elastic fibers as well as type III collagen amounts were decreased considerably in hypoxic cells treated with DHAP compared with the HG group.

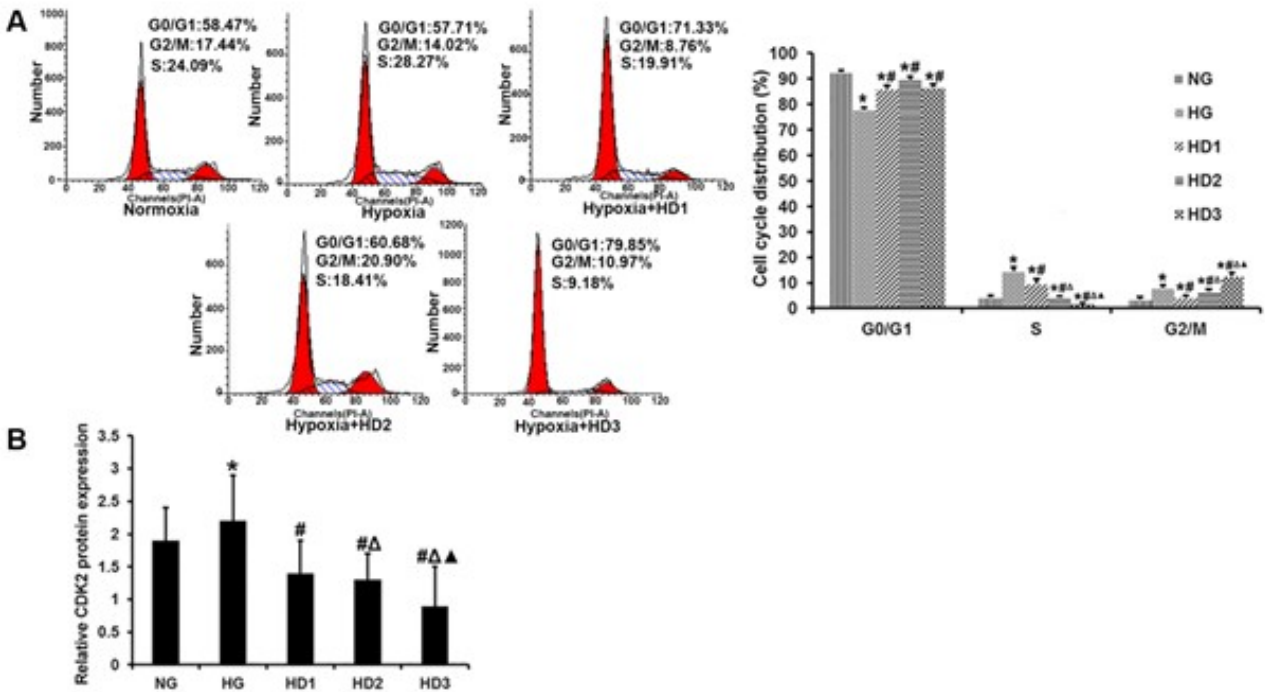


Fig. 3: Effects of DHAP on cell cycle distribution and CDK2 levels in HPASMCs under hypoxia. (A) Cell cycle distribution was assessed by flow cytometry after propidium iodide (PI) staining. (B) CDK2 protein expression was determined by Western blot, with β -actin as an internal control. Data are mean \pm SD. * P <0.05 vs. NG; # P <0.05 vs. HG; ΔP <0.05 vs. HD1; $\blacktriangle P$ <0.05 vs. HD2.

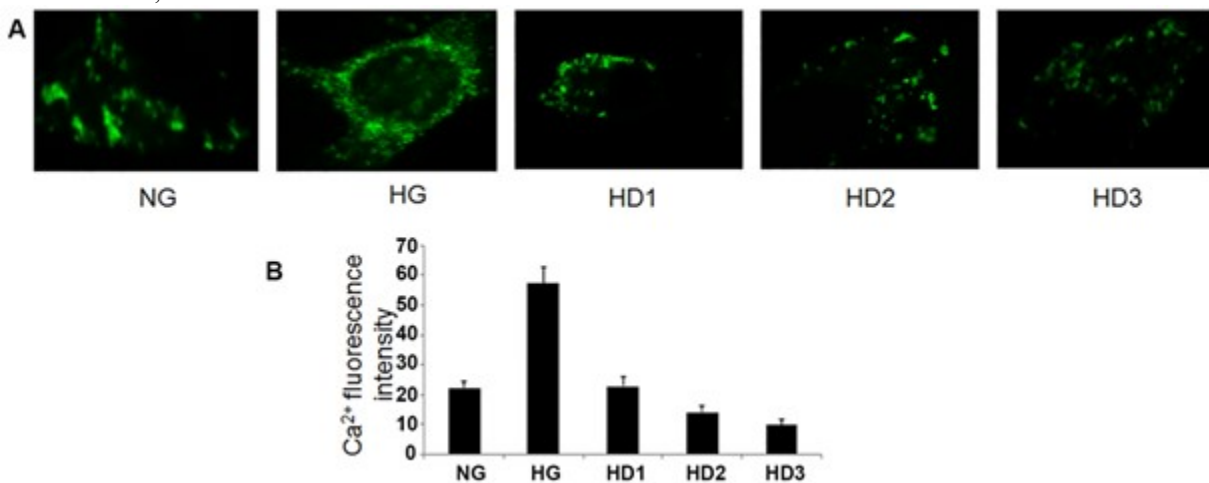


Fig. 4: Effects of DHAP on $[Ca^{2+}]_i$ in HPASMCs under hypoxia. (A) $[Ca^{2+}]_i$ was assessed by Fluo-3 AM. Typical laser scanning confocal microscopy images were acquired for the NG, HG, HD1, HD2 and HD3 groups. (B) Fluorescence intensities (FI). Data are mean \pm SD. * P <0.05 vs. NG; # P <0.05 vs. HG.

levels and subsequently increased both DNA synthesis and PCNA amounts in adult transgenic mouse hearts. Moreover, heart to body weight ratios are significantly increased in 2 day-old CDK2 transgenic neonatal mice (Liao *et al.*, 2001), suggesting that CDK2 participates in cell proliferation. In the present study, upon administration of DHAP, CDK2 levels were increased; this resulted in a cell cycle shift towards the S and G2/M phases, strongly suggesting that DHAP inhibits cell proliferation.

Ca^{2+} acts a central signal in HPASMC proliferation. It was previously shown that the transient receptor potential gene mediating Ca^{2+} entry through the store-operated channel (SOC) represents a critical mechanism in controlling intracellular Ca^{2+} levels ($[Ca^{2+}]_i$) in HPASMCs. Previous studies also demonstrated that PASMC migration is important in vascular remodeling occurring during HPH development (Shimizu *et al.*, 2013, Yang *et al.*, 2012). Although the mechanism underlying this phenomenon remains poorly understood, PASMC

proliferation and apoptosis have decisive effects on pulmonary vascular structure and function (Noureddine *et al.*, 2011). Increased $[Ca^{2+}]_i$ in PSMCs is an important stimulus for pulmonary vasoconstriction and vascular remodeling (Stenmark *et al.*, 2006). Elevated $[Ca^{2+}]_i$ and enhanced Ca^{2+} influx have been described in PSMCs from patients with idiopathic pulmonary arterial hypertension (IPAH) (Wang *et al.*, 2008, Yamamura *et al.*, 2012). The present study corroborated the above reports, showing that increased cytosolic K^+ and Ca^{2+} could lead to impaired apoptosis and increased cell proliferation (T. Wang *et al.*, 2005, Zhivotovsky and Orrenius, 2011).

Reactive oxygen species (ROS) are critical regulators of multiple pathophysiological events (Bolisetty and Jaimes, 2013). Mitochondria and NADPH oxidase are the main ROS sources in vessels (Sena and Chandel, 2012). Mounting evidence reveals the roles of ROS, especially hydrogen peroxide, as effect or molecules inducing $[Ca^{2+}]_i$ increase (Dikalov, *et al.*, 2012) and PSMC contraction by controlling multiple targets (Borer *et al.*, 2013). Therefore, ROS dysregulation is frequently observed in vascular diseases and may play a role in PAH. However, further study is required to delineate any possible regulatory effects of DHAP on these mechanisms.

The present study had several limitations. Indeed, exploration of the mechanisms involved in HPASMCM response to DHAP was very superficial. In addition, HPASMCs were harvested from lung cancer patients who underwent surgery and there is no guarantee that the metabolism of the harvested cells was unaffected by the process. More in-depth analyses are necessary to adequately unveil these mechanisms and to determine if DHAP could be used as an effective therapeutic agent against PAH.

CONCLUSION

In summary, the present study showed that DHAP could inhibit hypoxia-induced HPASMCM proliferation by reversing hypoxia associated shift from G0/G1 towards S and G2/M in the cell cycle and decreasing $[Ca^{2+}]_i$ in HPASMCs. These findings suggest DHAP could be used as a potential therapeutic agent against PAH.

REFERENCES

Bertoli C, Skotheim JM and De Bruin RA (2013). Control of cell cycle transcription during G1 and S phases. *Nat. Rev. Mol. Cell Biol.*, **14**(8): 518-528.
Bolisetty S and Jaimes EA (2013). Mitochondria and reactive oxygen species: Physiology and pathophysiology. *Int. J. Mol. Sci.*, **14**(3): 6306-6344.
Borer KE, Bailey SR, Harris PA and Elliott J (2013). Contractile responses of isolated equine digital arteries

under hypoxic or hyperoxic conditions *in vitro*: Role of reactive oxygen species and Rho kinase. *J. Vet. Pharmacol. Ther.*, **36**(3): 267-274.
Burger CD (2009). Pulmonary hypertension in COPD: A review and consideration of the role of arterial vasodilators. *Copd.*, **6**(2): 137-144.
Diaz-Guzman E and Mannino DM (2014). Epidemiology and prevalence of chronic obstructive pulmonary disease. *Clin. Chest. Med.*, **35**: 7-16.
Dikalov SI, Li W, Doughan AK, Blanco RR and Zafari AM (2012). Mitochondrial reactive oxygen species and calcium uptake regulate activation of phagocytic NADPH oxidase. *Am. J. Physiol. Regul. Integr. Comp. Physiol.*, **302**(10): R1134-1142.
Singh D, Agusti A, Anzueto A, Barnes PJ, Bourbeau J, Celli BR, Criner GJ, Frith P, Halpin DMG, Han M, López Varela MV, Martínez F, Montes de Oca M, Papi A, Pavord ID, Roche N, Sin DD, Stockley R, Vestbo J, Wedzicha JA and Vogelmeier C (2019). Global strategy for the diagnosis, management, and prevention of chronic obstructive lung disease: the gold science committee report 2019. *Eur. Respir. J.*, **53**(5):1900164.
Farman U, Wang DX and Deng J (1994). Effects of 3,4-dihydroxyacetophenone on hypoxic vasoconstriction in isolated pulmonary and basilar arterial rings. *J. Tongji. Med. Univ.*, **14**(4): 252-256.
Firth AL, Won JY and Park WS (2013). Regulation of Ca^{2+} signaling in pulmonary hypertension. *Korean J. Physiol. Pharmacol.*, **17**: 1-8.
Foo J, Landis SH, Maskell J, Oh YM, van der Molen T, Han MK, Mannino DM, Ichinose M and Punekar Y (2016). Continuing to Confront COPD International Patient Survey: Economic Impact of COPD in 12 Countries. *PLoS One*, **11**(14): e0152618.
Herbert LM, Resta TC and Jernigan NL (2018). RhoA increases ASIC1a plasma membrane localization and calcium influx in pulmonary arterial smooth muscle cells following chronic hypoxia. *Am. J. Physiol. Cell Physiol.*, **314**: C166-C176.
Islam SM, Furnat TD, Phuong NT, Mwingira U, Schacht K and Froschl G (2014). Non-communicable diseases (NCDs) in developing countries: A symposium report. *Global Health*, **10**: 81.
Jiang F, Guo N and Dusting GJ (2009). 3',4'-Dihydroxyflavonol down-regulates monocyte chemoattractant protein-1 in smooth muscle: role of focal adhesion kinase and PDGF receptor signalling. *Br. J. Pharmacol.*, **157**(4): 597-606.
Gregory D Lewis, Debby Ngo, Anna R Hemnes, Laurie Farrell, Carly Damos, Paul P Pappagianopoulos, Bishnu P Dhakal, Amanda Souza, Xu Shi, Meredith E Pugh, Arkadi Beloiartsev, Sumita Sinha, Clary B. Clish and Robert E. Gerszten. (2016). Metabolic profiling of right ventricular-pulmonary vascular function reveals circulating biomarkers of pulmonary hypertension. *J. Am. Coll. Cardiol.*, **67**(2): 174-189.
Liao HS, Kang PM, Nagashima H, Yamasaki N, Usheva A

- and Ding B (2001). Cardiac-specific overexpression of cyclin-dependent kinase 2 increases smaller mononuclear cardiomyocytes. *Circ. Res.*, **88**(4): 443-450.
- Lin C, Zhang Z and Xu Y (1995). Therapeutical mechanism of 3,4 dihydroxyacetophenone in treating chronic obstructive pulmonary disease. *Zhonghua Jie He He Hu Xi Za Zhi.*, **18**(2): 97-98.
- Lin CL (2008). 3,4-dihydroxyacetophenone inhibits proliferation of human pulmonary artery smooth muscle cells induced by focal adhesion kinase. *Zhongguo Ying Yong Sheng Li Xue Za Zhi.*, **24**(4): 486-487.
- Magne J, Pibarot P, Sengupta PP, Donal E, Rosenhek R and Lancellotti P (2015). Pulmonary hypertension in valvular disease: A comprehensive review on pathophysiology to therapy from the HAVEC Group. *JACC Cardiovasc Imaging.*, **8**: 83-99.
- McLaughlin VV, Shah SJ, Souza R and Humbert M (2015). Management of pulmonary arterial hypertension. *J. Am. Coll Cardiol.*, **65**(8): 1976-1997.
- Morgan KG, Gangopadhyay SS (2001). Invited review: Cross-bridge regulation by thin filament-associated proteins. *J. Appl. Physiol.*, **91**(2): 953-962.
- Noureddine H, Gary-Bobo G, Alifano M, Marcos E, Saker M and Vienney N (2011). Pulmonary artery smooth muscle cell senescence is a pathogenic mechanism for pulmonary hypertension in chronic lung disease. *Circ. Res.*, **109**(5): 543-553.
- Park SY, Lee CY, Kim C, Jang SH, Park YB and Park S (2015). One-year prognosis and the role of brain natriuretic peptide levels in patients with chronic cor pulmonale. *J. Korean Med. Sci.*, **30**(4): 442-449.
- Polverino F, Celli BR and Owen CA (2018). COPD as an endothelial disorder: Endothelial injury linking lesions in the lungs and other organs? (2017 Grover Conference Series). *Pulm Circ.*, **8**(1): 2045894018758528.
- Sena LA and Chandel NS (2012). Physiological roles of mitochondrial reactive oxygen species. *Mol. Cell*, **48**(2): 158-167.
- Shimizu T, Fukumoto Y, Tanaka S, Satoh K, Ikeda S and Shimokawa H (2013). Crucial role of ROCK2 in vascular smooth muscle cells for hypoxia-induced pulmonary hypertension in mice. *Arterioscler. Thromb. Vasc. Biol.*, **33**(12): 2780-2791.
- Smith KA, Voirit G, Tang H, Fraidenburg DR, Song S, Yamamura H, Yamamura A, Guo Q, Wan J, Pohl NM, Tauseef M, Bodmer R, Ocorr K, Thistlethwaite PA, Haddad GG, Powell FL, Makino A, Mehta D and Jason. Yuan XJ (2015). Notch Activation of Ca²⁺ Signaling in the Development of Hypoxic Pulmonary Vasoconstriction and Pulmonary Hypertension. *Am. J. Respir Cell Mol. Biol.*, **53**(3): 355-367.
- Stenmark KR, Fagan KA and Frid MG (2006). Hypoxia-induced pulmonary vascular remodeling: Cellular and molecular mechanisms. *Circ. Res.*, **99**(7): 675-691.
- Sue S and Zane N (1987). The role of culture and cultural techniques in psychotherapy. A critique and reformulation. *Am. Psychol.*, **42**(1): 37-45.
- Sun W and Chan SY (2018). Pulmonary Arterial Stiffness: An early and pervasive driver of pulmonary arterial hypertension. *Front Med (Lausanne)*; **5**(5): 204.
- Ullah F, Wang DX, Ming Z and Yu SB (1995). Effects of 3,4-dihydroxyacetophenone (3,4-DHAP) on hypoxic pulmonary and systemic vascular response in dogs. *J. Tongji. Med. Univ.*, **15**(1): 26-30.
- Wang C, Wang J, Zhao L, Wang Y, Liu J and Shi L (2008). Sildenafil inhibits human pulmonary artery smooth muscle cell proliferation by decreasing capacitative Ca²⁺ entry. *J. Pharmacol. Sci.*, **108**(1): 71-78.
- Wang T, Zhang ZX and Xu YJ (2005). Effect of mitochondrial KATP channel on voltage-gated K⁺ channel in 24 hour-hypoxic human pulmonary artery smooth muscle cells. *Chin. Med. J.*, **118**(1): 12-19.
- Wilson JL, Yu J, Taylor L and Polgar P (2015). Hyperplastic growth of pulmonary artery smooth muscle cells from subjects with pulmonary arterial hypertension is activated through JNK and p38 MAPK. *PLoS One*, **10**(4): e0123662.
- Yamamura A, Guo Q, Yamamura H, Zimnicka AM, Pohl NM and Smith KA (2012). Enhanced Ca²⁺-sensing receptor function in idiopathic pulmonary arterial hypertension. *Circ. Res.*, **111**(4): 469-481.
- Yang Q, Lu Z, Ramchandran R, Longo LD and Raj JU (2012). Pulmonary artery smooth muscle cell proliferation and migration in fetal lambs acclimatized to high-altitude long-term hypoxia: Role of histone acetylation. *Am. J. Physiol. Lung Cell. Mol. Physiol.*, **303**(11): L1001-1010.
- Zangiabadi A, De Pasquale CG and Sajkov D (2014). Pulmonary hypertension and right heart dysfunction in chronic lung disease. *Biomed. Res. Int.*, pp.739674.
- Zhivotovsky B and Orrenius S (2011). Calcium and cell death mechanisms: A perspective from the cell death community. *Cell Calcium*, **50**(3): 211-221.